BET SHEMESH ENGINES

AIJES 2022

Mechanical Properties, Metallurgical Characteristics and Anisotropy of Additive Manufacturing of 316L

Presented by **D. Moreno**

Y. Nahmana, O. Nafman, O. Kam, B. Wolfman, A.Y. Cohen and M. Shapira

Beth Shemesh Engines LTD, FAA&EASA, 1 Virginia Ave., Beth Shemesh, ISRAEL

Introduction

- **Additive manufacturing (AM) presents new challenge the achievement of the basic mechanical properties of alloys**
- **The AM process involved many aspects which include thermal phase transformation during a transiently process according to the thermodynamic roles of the metal components**
- **Austenite 316L stainless steel produced by AM demonstrate good ductility and high yield strength - higher than that obtained with annealed 316L in addition to some preferred orientation affecting the mechanical properties**
- **This anisotropy is attributed to the changes in the microstructure**

BET SHEMESH ENGINES

AIJES 2022

Schematic demonstrating the major processing parameters influencing AM results

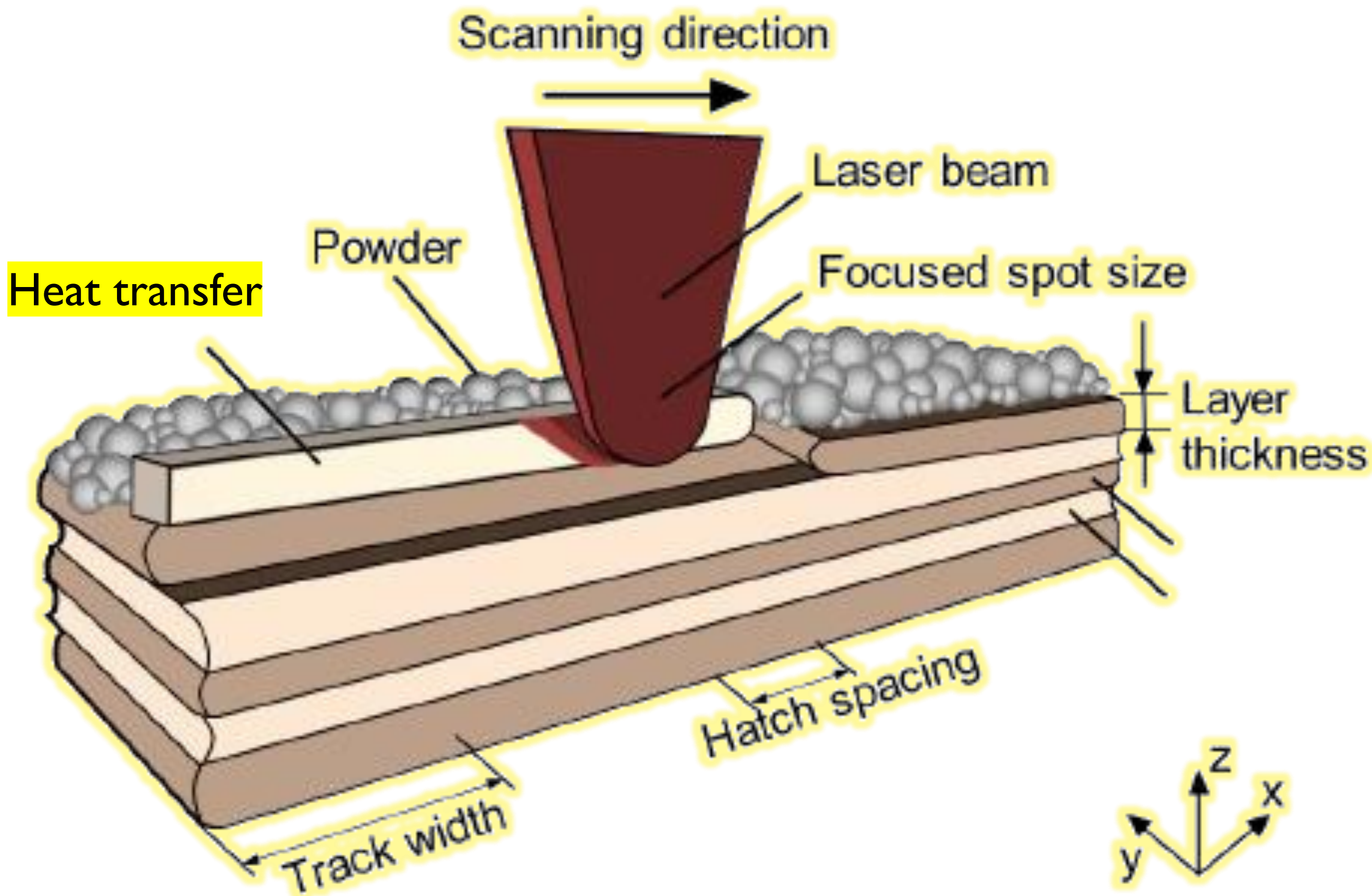

Experimental

Sample Preparation:

- 400-watt Yb(Ytterbium)-fiber laser with high beam quality spot, good resolution and good precision was used in the present work.
- The SS316L powder with a generic particle size of 20–65µm, spherical shape was used.
- Samples for mechanical properties characterization were printed in three different directions;
  - 0° (perpendicular to the printer beam),
  - 90° (perpendicular to the feed layer or parallel to the printer beam)
  - and 45° between them.
- The samples were machined to dog-bone tensile samples according to the following dimensions: 1/2-13 UNC -2A thread, 6.5mm diameter , 37mm length gage and total length of 86mm.

Sample Orientation (schematic)

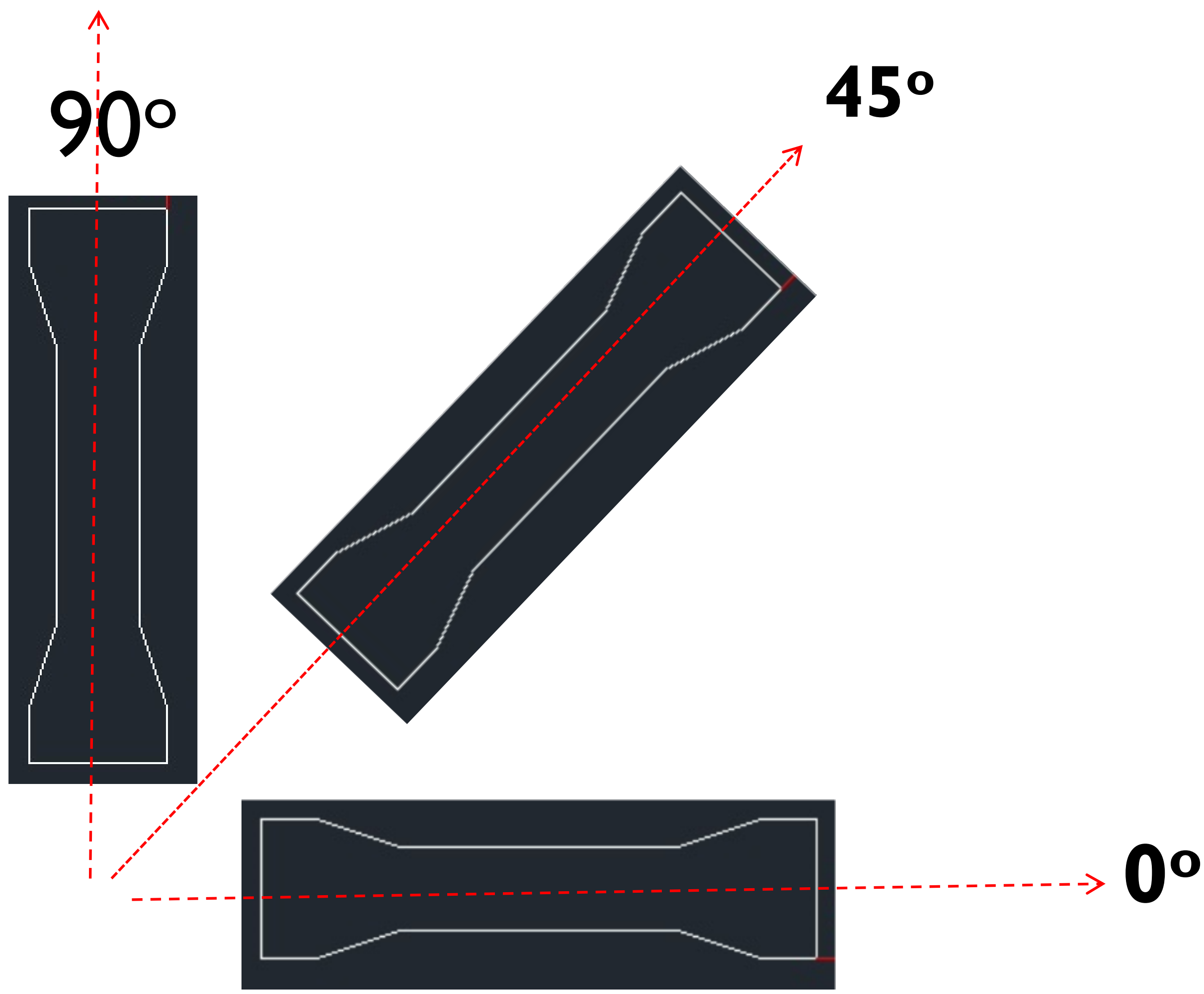

Experimental – cont’

Mechanical Properties

- The mechanical properties were measured in load control mode at 0.005 mm/min. rate up to the yield stress value and at 1.00 mm/min
- The tensile test was carried out with an Instron 5982 test machine at room temperature.

Characterization

- SEM fractography, EDX analysis of the fracture and optical cross section of the samples along the stress tension after the failure were carried out

BET SHEMESH ENGINES

AIJES 2022

Composition – spec. variations

	SLM		EOS-M290		GE		ASTM A269/276	
Indicative value (wt%)	**Min**	**Max**	**Min**	**Max**	**Min**	**Max**	**Min**	**Max**
Fe	Balance	Balance	Balance	Balance	Balance	Balance	Balance	Balance
Cr	16	18	17	**19**	16.5	18	16	18
Ni	10	14	13	15	10	13	10	15
Mo	2	3	2.25	3	2	2.5	2	3
Mn	0	2	0	2	0	2	0	2
Si	0	1	0	0.75	0	1	0	1
P	0	0.0045	0	0.025	0	0.0045	0	0.045
S	0	0.03	0	0.01	0	0.03	0	0.03
C	0	0.03	0	0.03	0	0.03	0	0.035
N	0	0.1	0	0.1	0	0	0.1	0.16

BET SHEMESH ENGINES

AIJES 2022

Composition

316L corrosion resistant steel spec and results (#J6W1)

Powder Chemical Composition, EDS measurement (weight percent)

Forged bar – ASTM A276/A276M-17 type 316L annealed

		Fe	Cr	Ni	Mo	C	N	Mn	Si
ASTM A276	Min.	balance	16	10	2				
	Max	balance	18	14	3	0.03	0.10	2	0.75
	Printed EDS*	balance	18	11.20	2.78				
	Wrought bar	balance	16.63	10.08	2.03	0.015	0.042	1.30	0.41

Powder Morphology for 316L St. Steel Powder

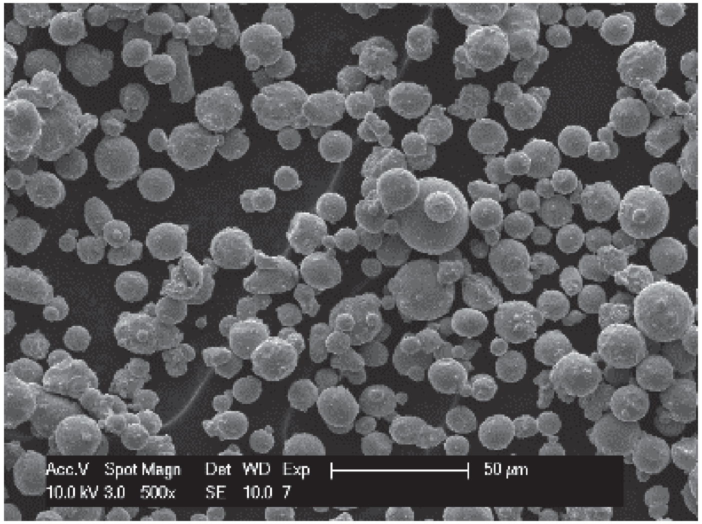

3D Systems

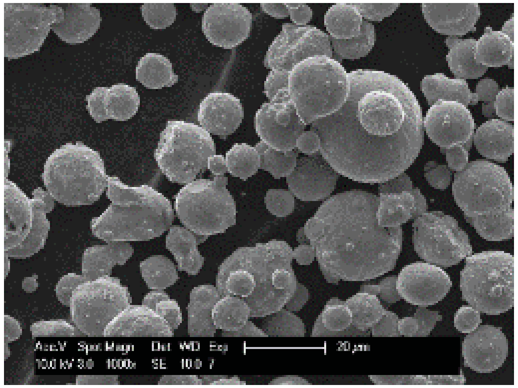

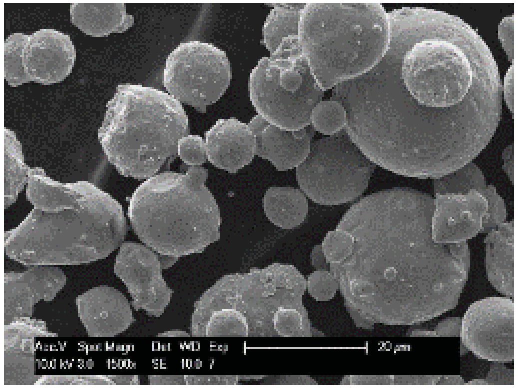

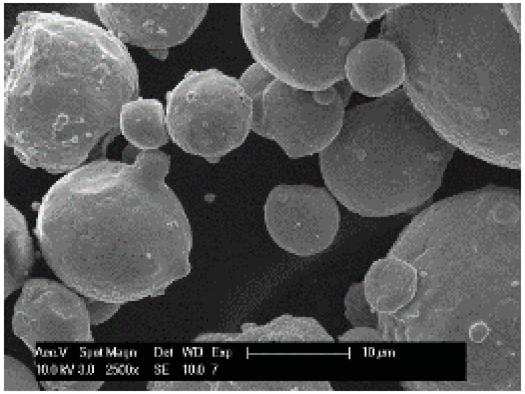

BET SHEMESH ENGINES

AIJES 2022

Stress – Strain Plot - Results

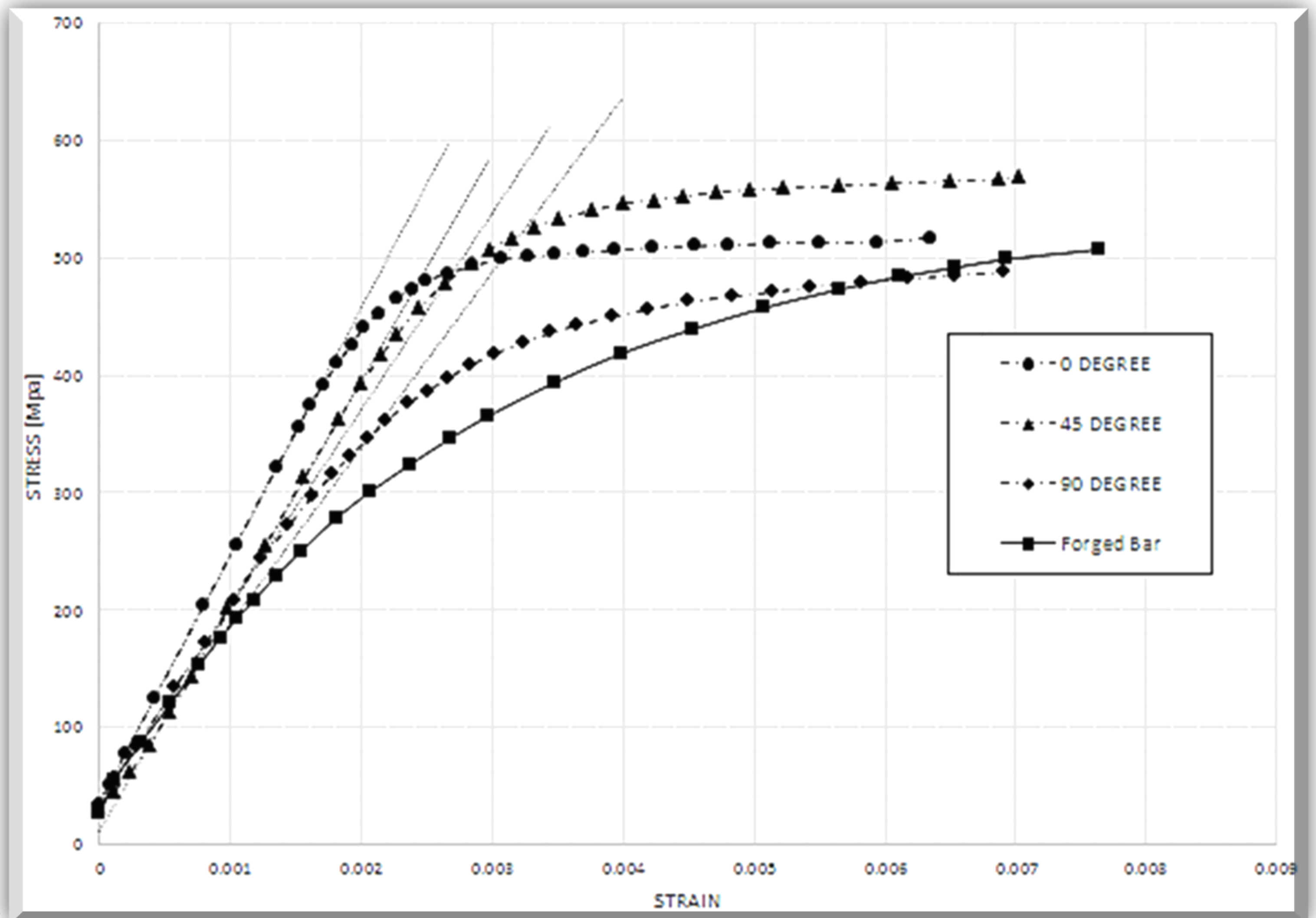

Mechanical properties values

Test No.	Specimen	Machine BS No.	D_0 mm	L_{04D} mm	L_{f4D} mm	UTS MPa	Yield (0.2% Offset	Elong. (4D)%	Youngs Modulus (GPa)	Amb. Temp °C	Fracture Location	Conform
T-32296	45°	17666	6.260	24.901	36.310	669	554	45.8	175	24.4	In gauge length	OK
T-32297	90°	17666	6.360	24.972	38.706	573	460	55.0	150	24.6	In gauge length	OK
T-32339	0°	17666	6.330	24.934	37.986	683	508	52.3	189	23.1	In gauge length	OK
*T-32526 (M-211799)	ASTM BAR	17666	6.350	25.004	40.627	645	438	62.5	153	23.5	In gauge length	OK
	Req. min		-	-	-	**550**	**290**	**30**	**150-200**	-	-	-

Ref MCL REP. M21108R1

Fracture Necks

Optical metallogra*phy* comparison of the necks obtained in the different samples.

a. Initially brittle and then ductile for the 0º

b. Almost ductile for the 45º

c. Ductile flow neck for the 90º and

d. Very ductile obtained in the forged and annealed sample

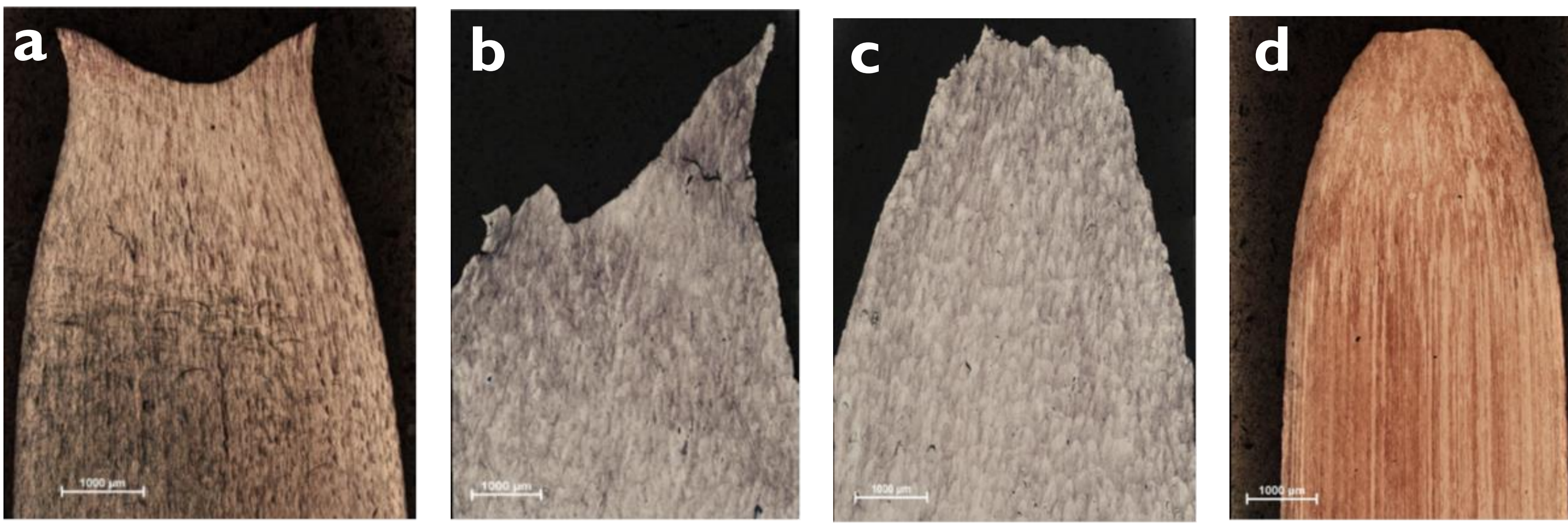

SEM Images of the fracture surface

SEM image comparison of the fracture surface necks obtained in the different samples.
The plastic deformation of the printed sample perpendicular to the fed beam, 0º orientation presented in (a), 90º oriented in (c,) and the forged bar, heat-treated sample in (d) show similar behavior during failure.
The 45º oriented sample shows deformation in two modes; normal stresses and shear stresses (b).

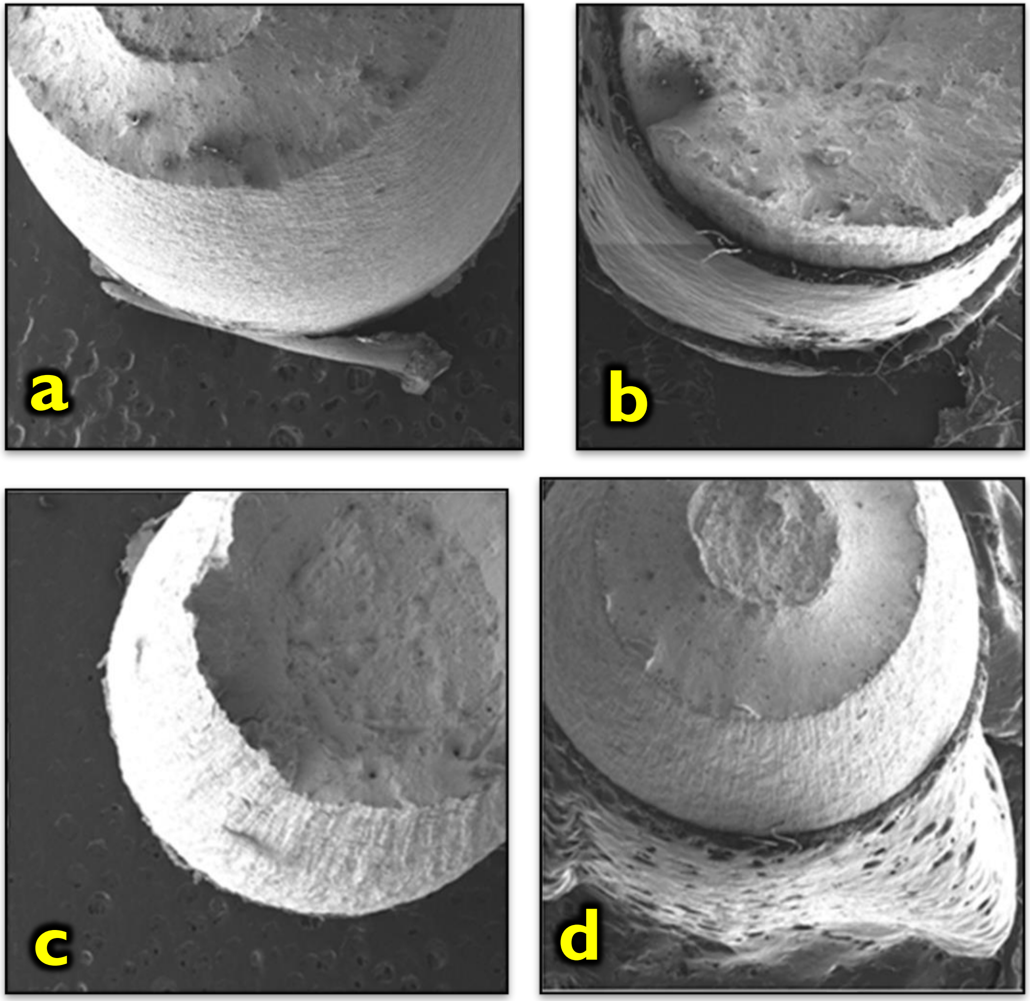

Dimple Structures

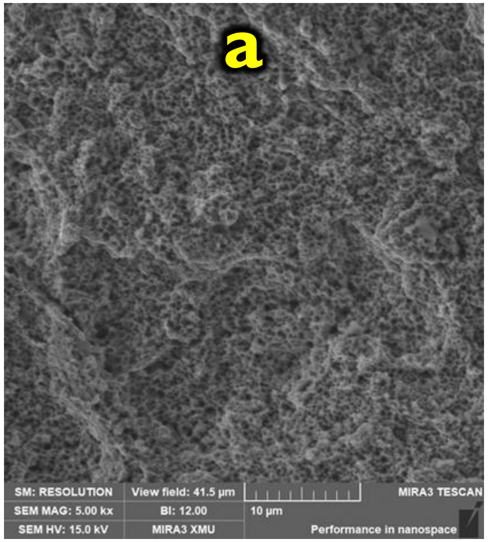

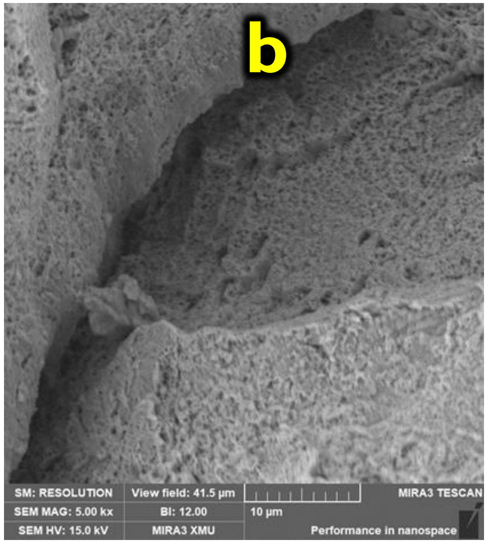

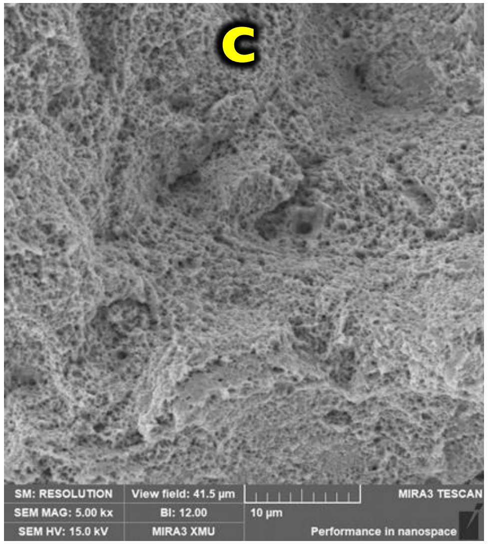

Comparison SEM images of the fracture surfaces obtained in the different samples show ductile dimples characteristic at sub-micron size for the 0º (a), 45º (b), 90º (c) and very ductile obtained in the BAR annealed sample with large dimples (d).

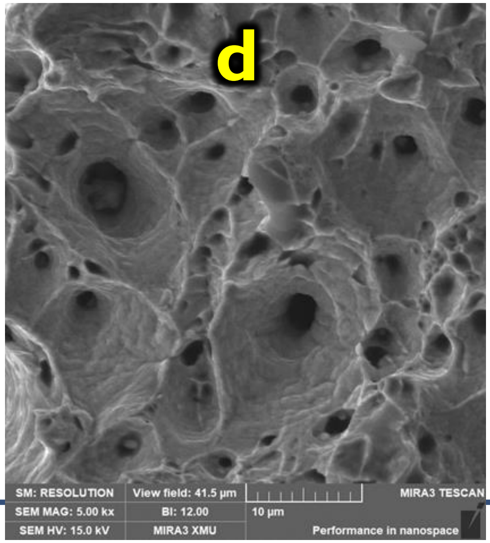

Voids, Slips and Twins

Comparison SEM images of the magnified polished surfaces in figure a-d, not far from the fracture, show combination of multi-voids, slips and twins deformation in printed samples at 45º (b), 90º (c) and the forged bar heat treated sample (d).
Sample printed in 0º (a) present multi-voids only after deformation close to the fracture.

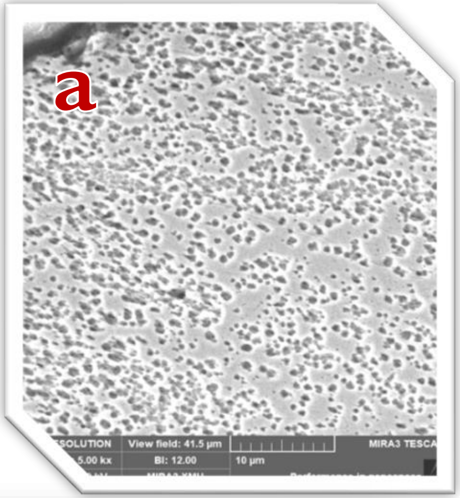

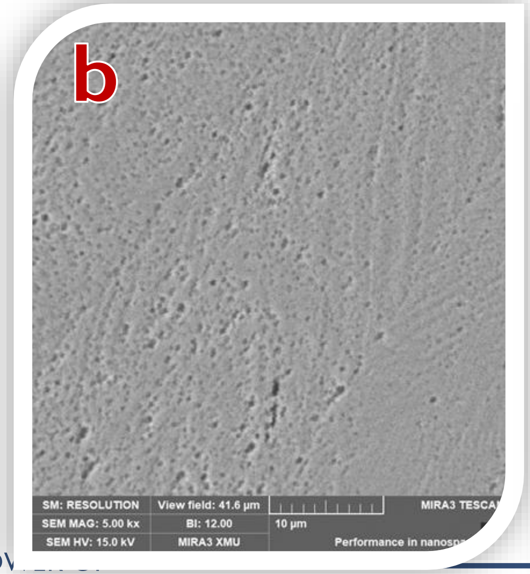

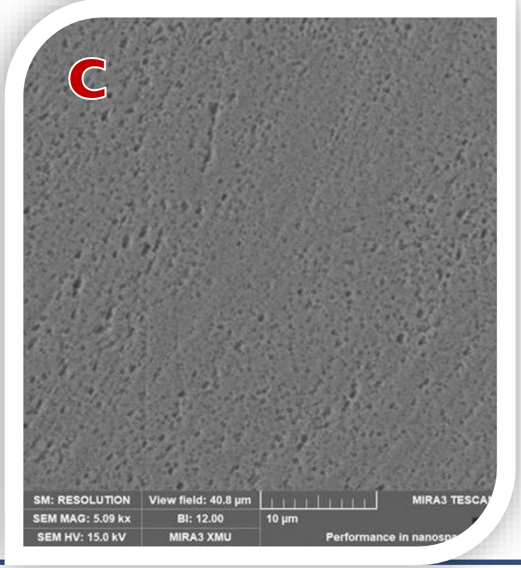

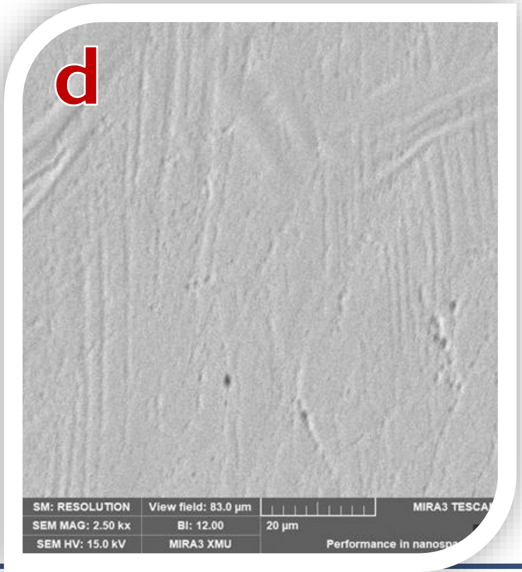

Perimeter Near the Fracture

SEM image (x400) of the sample perimeter and the fracture surface in the same picture (arrows show the edge between perimeter gage length surface close to the neck and the fracture area), images show slip band at different directions and levels.

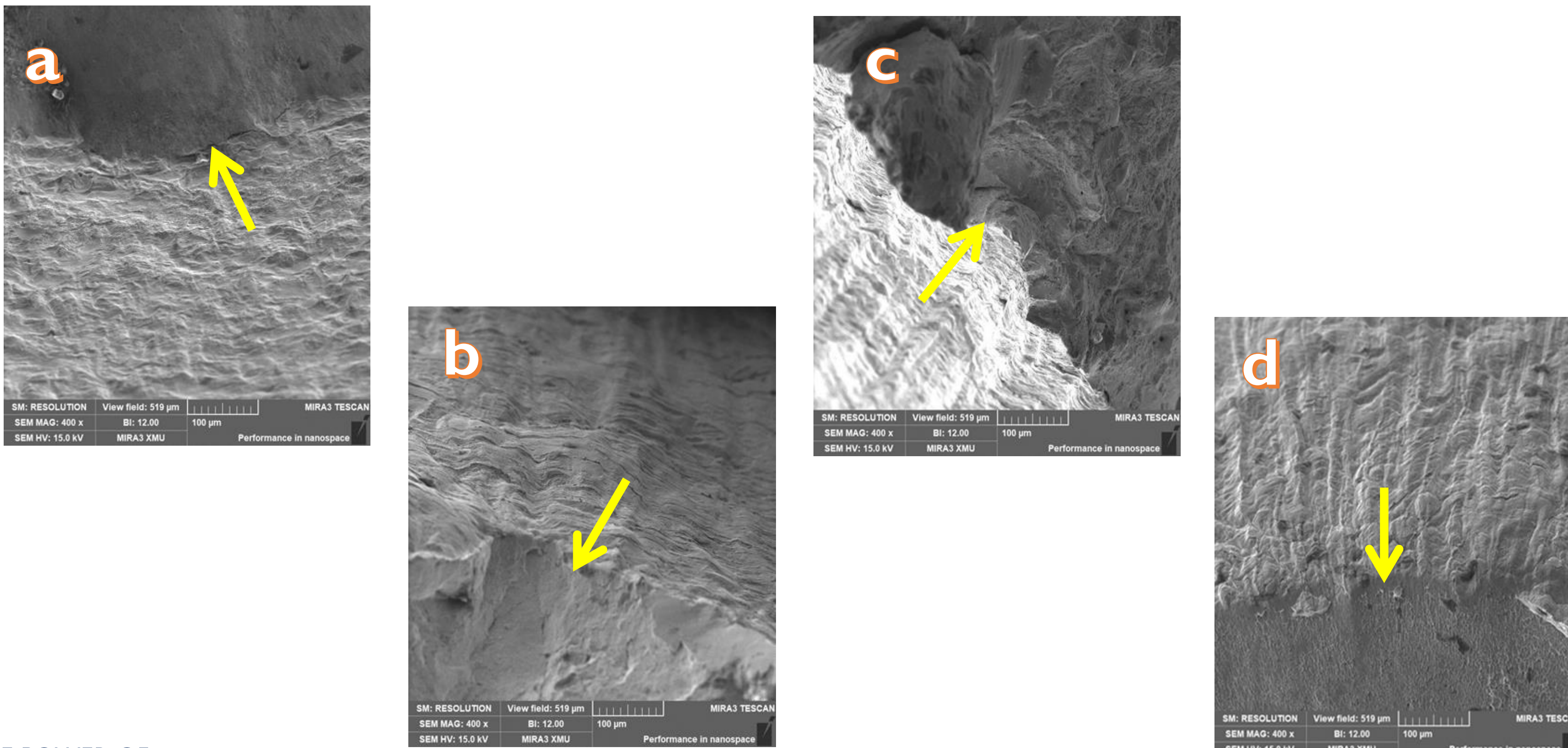

Supporting Results Samples (I)

Deformation behavior and irradiation tolerance of 316 L stainless steel fabricated by direct energy deposition

Ching-Heng Shiau a,b , Michael D. McMurtrey a , Robert C. O'Brien a , Nathan D. Jerred a , Randall D. Scott a , Jing Lu c , Xinchang Zhang d , Yun Wang e , Lin Shao b , Cheng Suna, ∗

- **Results reported at**
- **Show similar characterist**

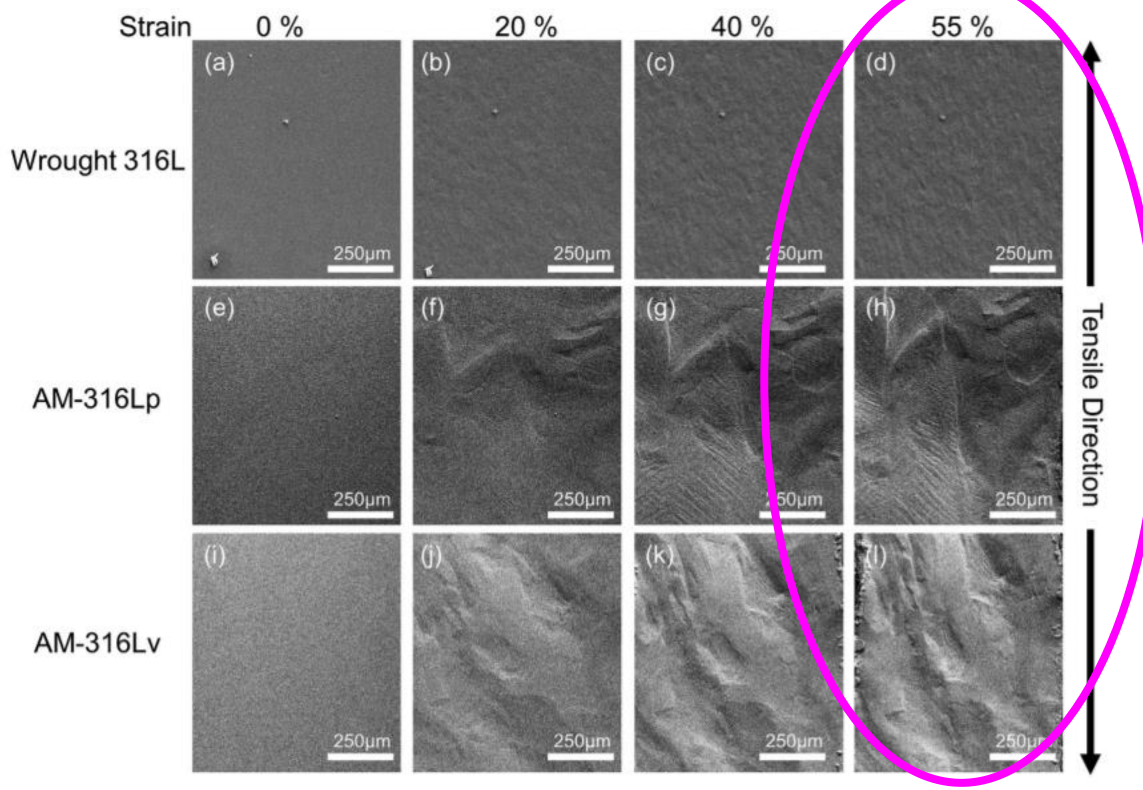

Fig. 7. In situ tensile test of wrought and AM-316 L stainless steels at room temperature in SEM. Secondary electron micrographs of wrought 316 L, AM-316 Lp, and AM-316 Lv at the strain levels of 0%, 20%, 40%, and 55%, showing the surface roughening on the surface closed to the necking region in AM-316 L.

AM-316 Lv and AM-316 Lp denote the specimens vertical and parallel to the substrate, respectively.

Discussion

One definition of heat input is the "Energy Density" (E)

$$E = \frac{P}{v * h * t}$$

where P is the laser power in watts,
v is the travel speed in mm/s,
h is the hatch spacing in mm, and t is the layer thickness in mm.

Grain growth Interactions between fluid flow, thermal gradient, and crystal properties control grain growth

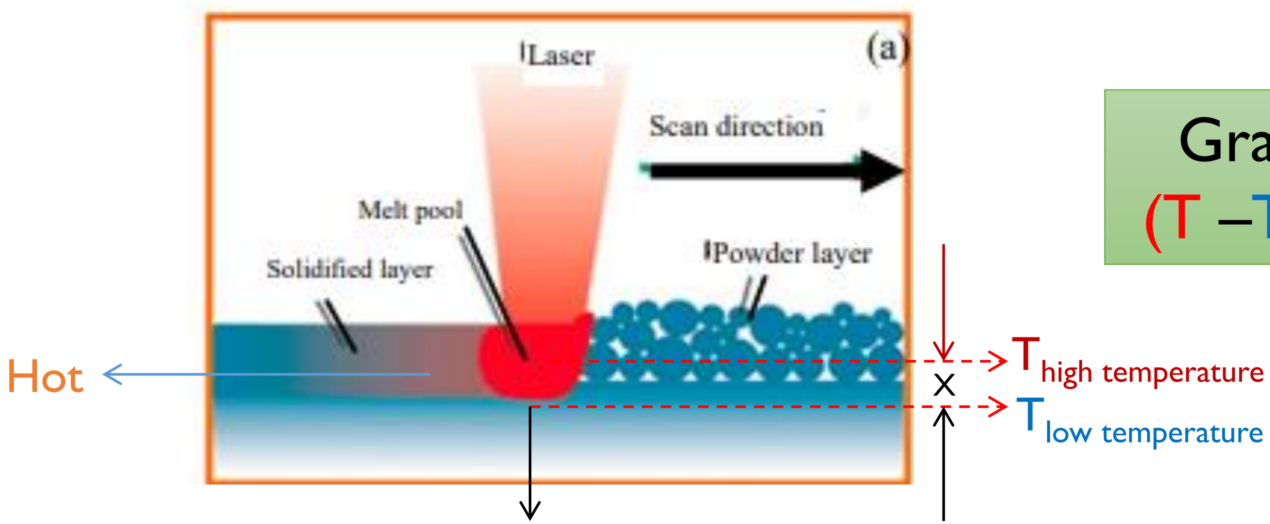

Gradient

(T –T)/x = ΔG

Heat Flow and Growth Direction

Temperature Gradient and Rate

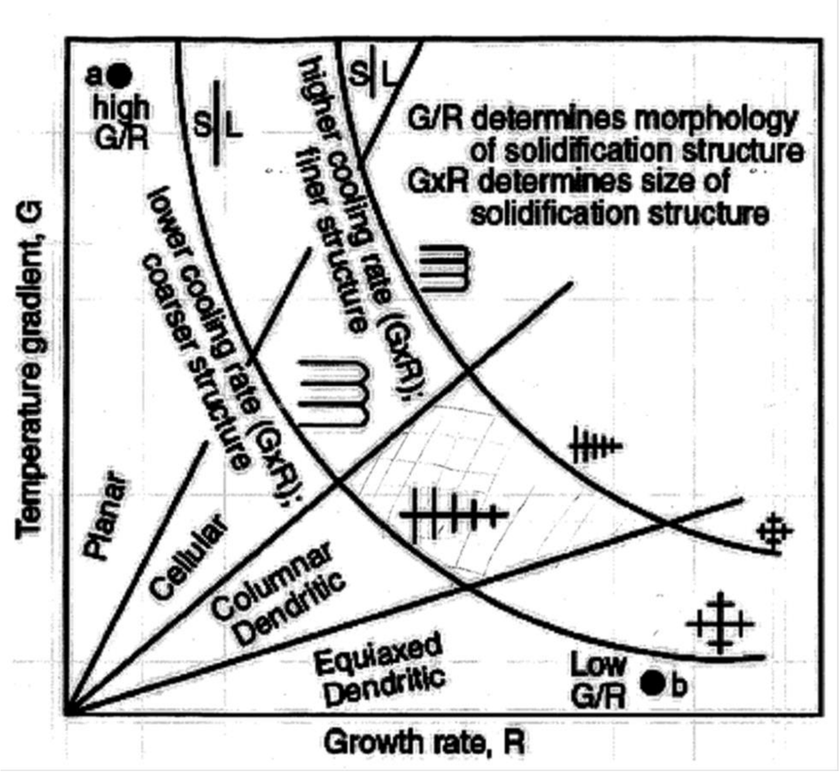

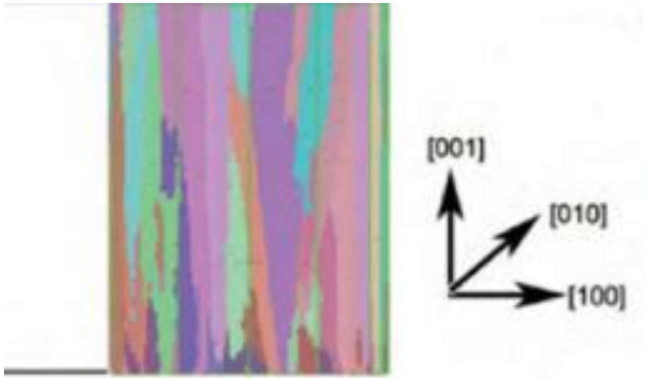

FCC Growth

Crystal structure	Preferred growth direction	Examples
FCC	$\langle 100 \rangle$	Al, Cu, Ni, γ-Fe
BCC	$\langle 100 \rangle$	δ-Fe, Succinonitrile (SCN), NH_4Cl (CsCl-type)
Tetragonal	$\langle 110 \rangle$	Sn
HCP	$\langle 10\bar{1}0 \rangle$	Zn, H_2O

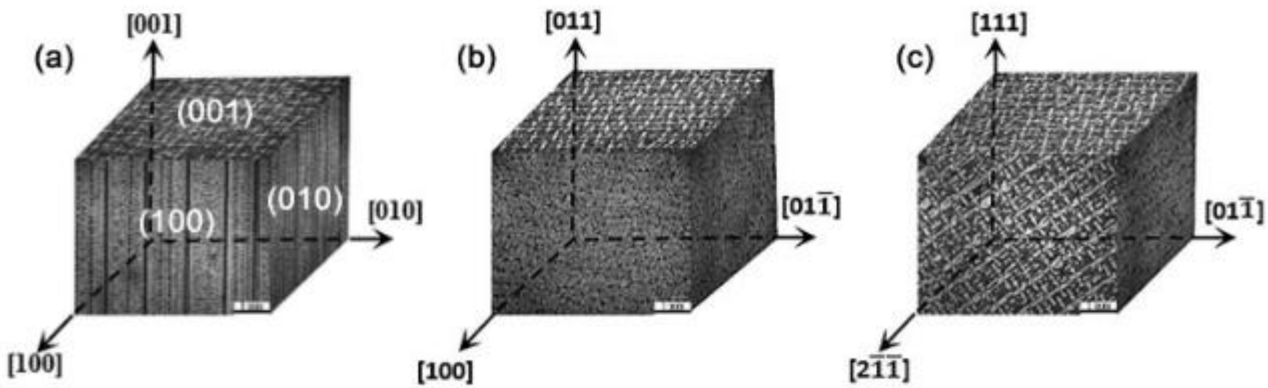

Distribution Growth

Most Grains at [001] directions

Some Grains close to [111]

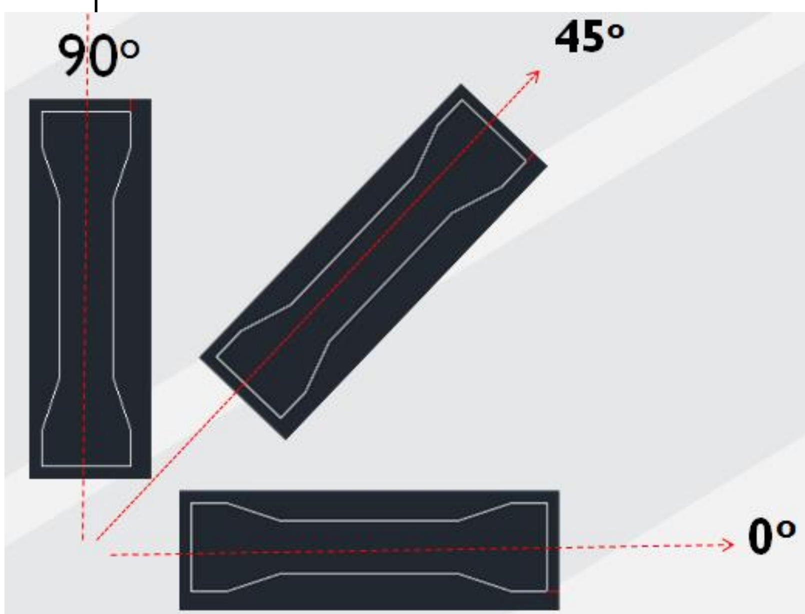

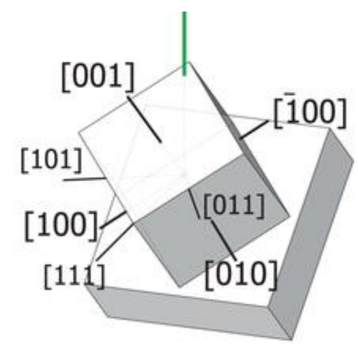

Most of the Grains between [101] and [010]

ANISOTROPY OF MECHANICAL PROPERTIES OF SINGLE CRYSTALS IN A FCC ALLOY – Similar Effects to be considered

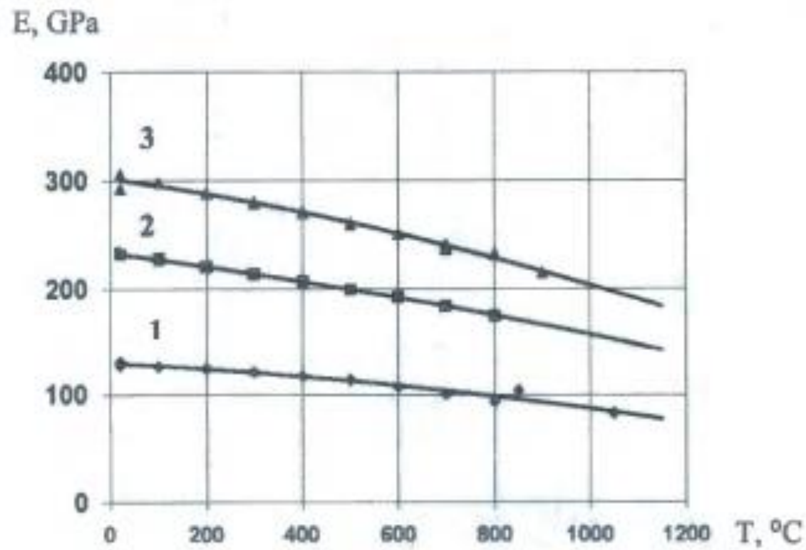

Temperature dependence of Young modulus in single crystals of 1- <001>, 2- <011>, 3- <111> orientations

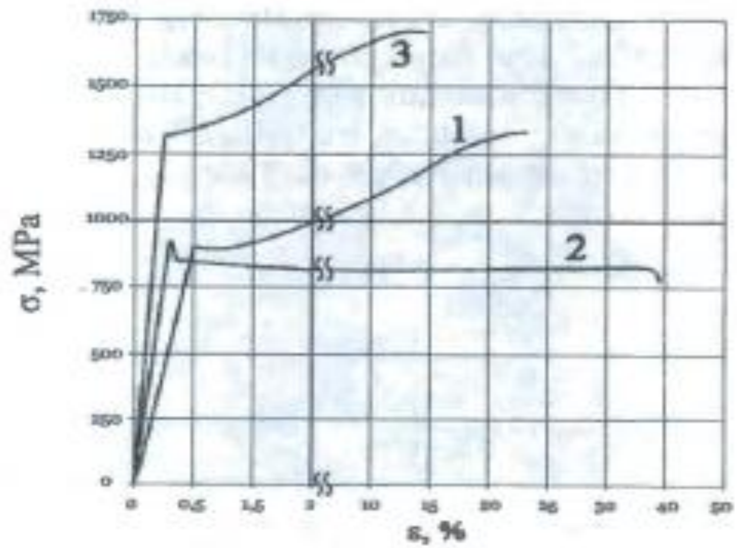

Deformation diagrams of the investigated alloy with crystallographic orientations, close to <001>, <011> and <111> at temperatures: 20°C

Ref - ANISOTROPY OF MECHANICAL PROPERTIES OF SINGLE CRYSTALS IN FOURTH GENERATION NI-BASED SUPERALLOY
I.L. Svetlov, N.V. Petrushin, D.V. Shchegolev, K.K. Khvatskiy
All-Russian Scientific-Research Institute of Aviation Materials (VIAM), Moscow, Russia
91 " Liege Conference: Materials for Advanced Power Engineering 2010

Conclusions

- Mechanical properties anisotropy was found in the AM printed samples. This should be considered while designing AM parts
- This anisotropy may be attributed to the changes in the microstructure and fractures modes presented.
- The mechanical properties of the AM printed samples in all direction:
  - Young Modulus, yield stress and UTS, present better values in comparison to the forged sample.
  - The elongation of the forged and heat-treated sample is higher and presents a softer material in comparison to the AM printed samples.
- Young's modulus of the lowest value at 90° is attributed to the preferred orientation grow in the AM samples by the feed up of the layers, the thermal process and the solidification front.
- These results are consistent with the basic theory and the obtained results in this study.